Article

Temperature-Induced Self-Pinning and Nanolayering of AuSi Eutectic Droplets

Nicola Ferralis, Roya Maboudian, and Carlo Carraro

J. Am. Chem. Soc., **2008**, 130 (8), 2681-2685 • DOI: 10.1021/ja7101983

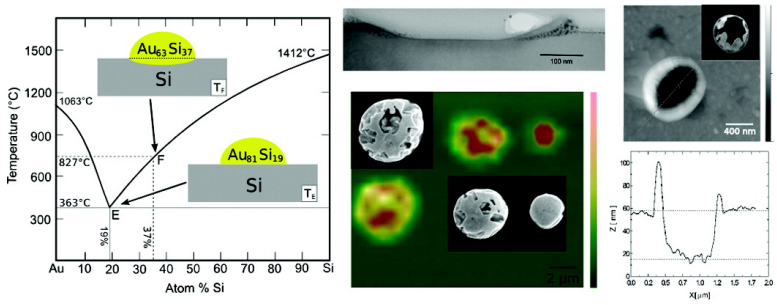

More About This Article

Additional resources and features associated with this article are available within the HTML version:

- Supporting Information
- Links to the 1 articles that cite this article, as of the time of this article download
- Access to high resolution figures
- Links to articles and content related to this article
- Copyright permission to reproduce figures and/or text from this article

View the Full Text HTML

J|A|C|S
ARTICLES
Published on Web 02/02/2008

Temperature-Induced Self-Pinning and Nanolayering of AuSi Eutectic Droplets

Nicola Ferralis, Roya Maboudian,* and Carlo Carraro

Department of Chemical Engineering, University of California, Berkeley, California 94720

Received November 9, 2007; E-mail: maboudia@berkeley.edu

Abstract: A process for self-pinning of AuSi eutectic alloy droplets to a Si substrate, induced by a controlled temperature annealing in ultrahigh vacuum, is presented. Surface pinning of AuSi 3D droplets to the Si substrate is found to be a consequence of the readjustment in the chemical composition of the droplets upon annealing, as required to maintain thermodynamic equilibrium at the solid−liquid interface. Structural and morphological changes leading to the pinning of the droplets to the substrate are analyzed. Phase separation is observed upon cooling of the droplets, leading to the formation of amorphous Si-rich channels within the core and the formation of crystalline Si nanoshells on the outside. The mechanism leading to the pinning and surface layering provides new insight into the role of alloying during growth of silicon nanowires and may be relevant to the engineering of nanoscale Si cavities.

Introduction

A resurgence of interest in the interfacial properties of the alloyed Au−Si system has been driven in part by the remarkable catalytic properties of gold clusters and their potential applications in nanotechnology.[1−4] In spite of the simplicity of the bulk three-dimensional binary phase diagram, geometric confinement and bonding frustration bring about remarkable complexity in low-dimensional structures, as exemplified in two dimensions by the structural complexity of submonolayer Au on Si(111).[5−8]

Gold and silicon do not form stable crystalline bulk intermetallic compounds owing to the profound differences in the nature of the chemical bonding in the two solids, which frustrates the system. The existence of a deep eutectic (Figure 1a), the glassy nature of the Au-rich alloy, the unusual layering and surface crystallization observed in the bulk liquid alloy at eutectic composition,[3] and the mechanical weakness of the Au−Si interface[9] are all consequences of this frustration. In two dimensions and, more generally, under strong confinement, frustration is expected to lead to self-organization into mesoscopic patterns, an example of which is found in the Stranski−Krastanov growth mode of thick gold films, as they dewet the surface of silicon upon annealing.

In dewetting equilibrium, isolated drops of a simple liquid coexist with a thin (possibly submonolayer) adsorbed film, uniformly spread over the substrate.[10] Similarly the dewetting of thick gold films from the Si surface upon annealing is accompanied by the formation of a monolayer-thin film of gold silicide between droplets of Au−Si eutectic alloy (Figure 1b).[5] The binary nature of this alloy results in a complex structure of both the thin film and the nonwetting droplets. The nature of Au monolayer films on Si(111) has been well-characterized in ultrahigh vacuum studies.[6−8] In addition, studies of the wetting behavior of liquid 3D droplets as a function of temperature[11−12] indicate that a certain degree of mobility is present at low annealing temperature, due to nonequilibrium conditions imposed by a change in composition due to Si incorporation from surface steps. However pinning at surface steps has also been observed[13−14] and used to control the position of the islands on the surface.[15] In this work we provide strong evidence that surface pinning of AuSi 3D droplets to the Si substrate is a direct consequence of a necessary readjustment in the chemical composition of the droplets to maintain the equilibrium condition at the solid−liquid interface in the AuSi phase diagram and can be achieved regardless of the presence of surface steps (thus the label "self-pinning"). Such mechanism is obtained by a programmed temperature annealing.

Experimental Details

Gold films were deposited at room temperature by evaporation (Omicron EM3 evaporator; Au flux of 25 nA at 765 V; deposition rate

(1) Hannon, J. B.; Kodambaka, S.; Ross, F. M.; Tromp, R. M. *Nature* **2006**, *440*, 69−71.
(2) Campbell, C. T. *Science* **2004**, *306*, 234.
(3) Shpyrko, O. G.; Streitel, R.; Balagurusamy, V. S. K.; Grigoriev, A. Y.; Deutsch, M.; Ocko, B. M.; Meron, M.; Lin, B.; Pershan, P. S. *Science* **2006**, *313*, 77−80.
(4) Kodambaka, S.; Tersoff, J.; Reuter, M. C.; Ross, F. M. *Science* **2007**, *316*, 729−732.
(5) Le Lay, G.; Faurie, J. P. *Surf. Sci.* **1977**, *69*, 295.
(6) Nogami, J.; Baski, A. A.; Quate, C. F. *Phys. Rev. Lett.* **1990**, *65*, 1611−1614.
(7) Nagao, T.; Hasegawa, S.; Tsuchie, K.; Ino, S.; Voges, C.; Klos, G.; Pfnur, H.; Henzler, M. *Phys. Rev. B* **1998**, *57*, 10100.
(8) Nakajima, Y.; Voges, C.; Nagao, T.; Hasegawa, S.; Klos, G.; Pfnur, H. *Phys. Rev. B* **1997**, *55*, 8129.
(9) Ferralis, N.; Maboudian, R.; Carraro, C. *J. Phys. Chem. C* **2007**, *111*, 7508−7513.
(10) Cheng, E.; Cole, M. W.; Dupont-Roc, J.; Saam, W. F.; Treiner, J. *Rev. Mod. Phys.* **1993**, *65*, 557−567.
(11) Ressel, B.; Prince, K. C.; Heun, S.; Homma, Y. *J. Appl. Phys.* **2003**, *93*, 3886.
(12) Swiech, W.; Bauer, E.; Mundschau, M. *Surf. Sci.* **1991**, *253*, 283.
(13) Rota, A.; Martinez-Gil, A.; Agnus, G.; Moyen, E.; Maroutian, T.; Martenlian, B.; Megy, R.; Handbchen, M.; Beauvillain, P. *Surf. Sci.* **2006**, *600*, 1207−1212.
(14) Hibino, H.; Watanabe, Y. *Surf. Sci.* **2005**, *588*, L233−L238.

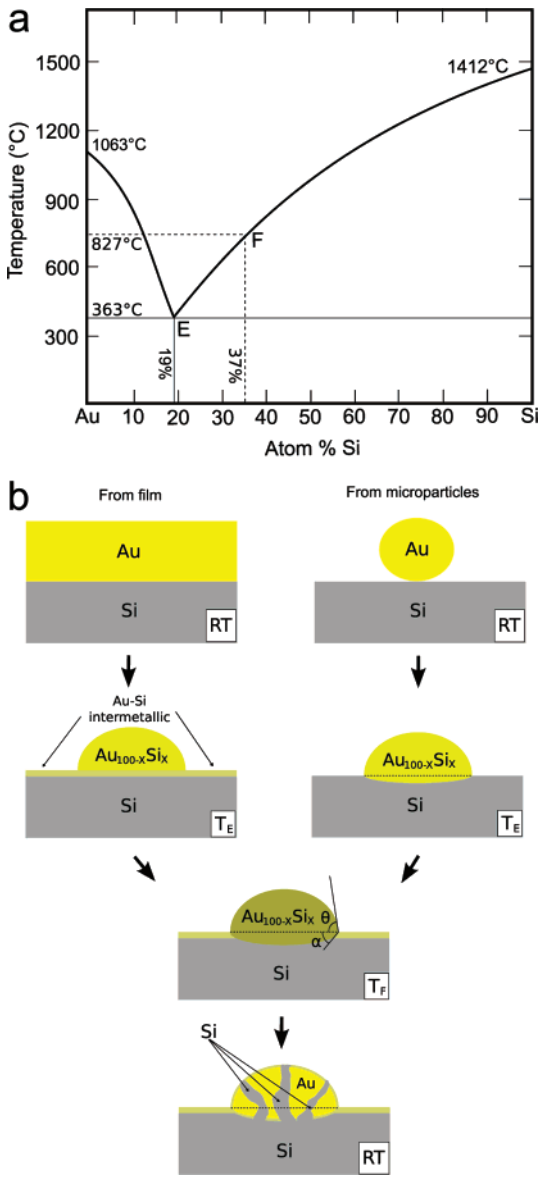

Figure 1. (a) Gold−silicon bulk phase diagram, indicating the eutectic point E at $T_E = 363$ °C and $X_E = 19\%$. Point F corresponds to the highest annealing temperature of 827° reached in our experiments. (b) Schematic representation of the evolution in composition and morphology of gold on a silicon surface upon annealing to T_E and T_F and subsequent quenching to room temperature, RT. Dewetting of a thick Au *film* on Si(111) (left) near the eutectic temperature (T_E) results in an alloyed droplet (with eutectic composition) in equilibrium with a highly structured thin film. The formation of depressions underneath the droplets ensues as they are annealed at higher temperatures (T_F), a consequence of the enrichment in the Si composition of the alloy. When one starts from microscopic Au *particles*, depressions form already at the eutectic temperature, by extracting Si from the substrate to reach the eutectic composition. Whether one starts with Au thick films or dispersed particles, after being cooled to room temperature, the droplets exhibit a thin Si outer nanoshell and Si channels inside the droplets. The percentage X of Si in the alloyed droplet (Au_{100-X} Si_X) varies from 19% at the eutectic to 37% at $T_F = 827$ °C.

~0.15 ML/min measured using the Au AES signal at 69 eV and Si AES signal at 92 eV). In some experiments, an alternative deposition method was used, by which gold microspheres (diameter 0.8−1.5 μm), previously mixed in nitrogen gas, were dispersed on H-terminated Si(111) surfaces. Single-crystal p-type Si(111) crystals were prepared as described elsewhere.[9] Samples were annealed in a UHV chamber (base pressure of 2×10^{-10} Torr), equipped with conventional rear-view low-energy electron diffraction (LEED, VG Microtech) and a cylindrical mirror analyzer for Auger electron spectroscopy (AES, PHI-Perkin-Elmer model 10-155). Surface morphology was characterized in air using a Digital Instruments Nanoscope IIIa atomic force microscope (AFM) operating in tapping mode (Ti−Pt-coated Si cantilever, force constant of 4.5 N/m, resonant frequency of 150 kHz, Q-factor of ~200). Cross-sectional TEM (Jeol 200CX) and SEM (Jeol 6490LV) were also used to investigate the surface morphology. Raman spectroscopy (JY Horiba LabRAM in backscattering configuration; excitation line provided by a HeNe laser through an Olympus BX41 confocal microscope) was used in conjunction with a high-resolution piezoelectric stage to obtain maps of stress and crystal structure. Selective etching of gold (4:1:40 KI:I_2:H_2O) or silicon (KOH etch solution at 80 °C) was performed on some samples ex situ.

Results and Discussion

In thermal equilibrium, the chemical composition of the liquid 3D alloy droplets follows the liquidus line, and hence, the alloy is enriched in Si upon heating, in order to achieve the equilibrium composition of the binary system (Figure 1a). This enrichment occurs by dissolution of the underlying substrate. Contrary to the suggestion that the process takes place in a layer-by-layer fashion, with dissolution of Si atoms into droplets as they move along step edges,[11] our experiments reveal that the droplets dig up for Si at localized sites.

Gold films, evaporated in ultrahigh vacuum onto clean Si(111) crystals and heated in UHV at the eutectic temperature T_E, turned into thin sheets of eutectic melt (alloy composition $Au_{81}Si_{19}$), which readily dewetted the surface, and formed liquid droplets with 3D eutectic composition over a background gold monolayer with 6×6 reconstruction. Some samples were further annealed to $T > T_E$ and then quenched to room temperature. Subsequently, both groups of samples were dipped ex situ in gold etch solution. Chemical (with AES) and structural analysis (with LEED) of both groups of samples after etching revealed a 2D AuSi intermetallic layer and $(\sqrt{3} \times \sqrt{3})$ surface reconstruction. However, analysis of surface topography revealed that while samples annealed at the eutectic temperature had a flat surface, those that were further heated showed pronounced circular depressions at the locations where the droplets resided before etching (schematically shown in Figure 1b). Figure 2a shows an atomic force micrograph of a sample annealed at 827 °C and quenched to room temperature (4 °C/s). Immersion of the sample in the iodine gold etch reveals the presence of depressions where the droplets once stood (Figure 2b,c). These depressions are also observed in cross-section transmission electron microscopy (Figure 2d).

The self-pinning process is independent of the dewetting of Au films while annealed at high temperatures: similar results were indeed obtained by annealing in UHV Au microdroplets (Alfa Aesar, 99.96% purity, diameter 0.8−1.5 μm) deposited onto a H-terminated Si(111) surface through a turbulent N_2 gas flow. In addition to the depressions in the sites previously occupied by the clusters, a circular silicon nanorim (approximately 25−30 nm high) surrounding the depressions can be observed in Figure 2b,d. Similar ring-shaped features were observed as a product of the nanomachining of silicon by gold-catalyzed oxidation.[16]

(15) Homma, Y.; Finnie, P.; Ogino, T.; Noda, H.; Urisu, T. *J. Appl. Phys.* **1999**, *86*, 3083−3088.

(16) Robinson, J.; Evans, P.; Liddle, J.; Dubon, O. *Nano Lett.* **2007**, *7*, 2009−2013.

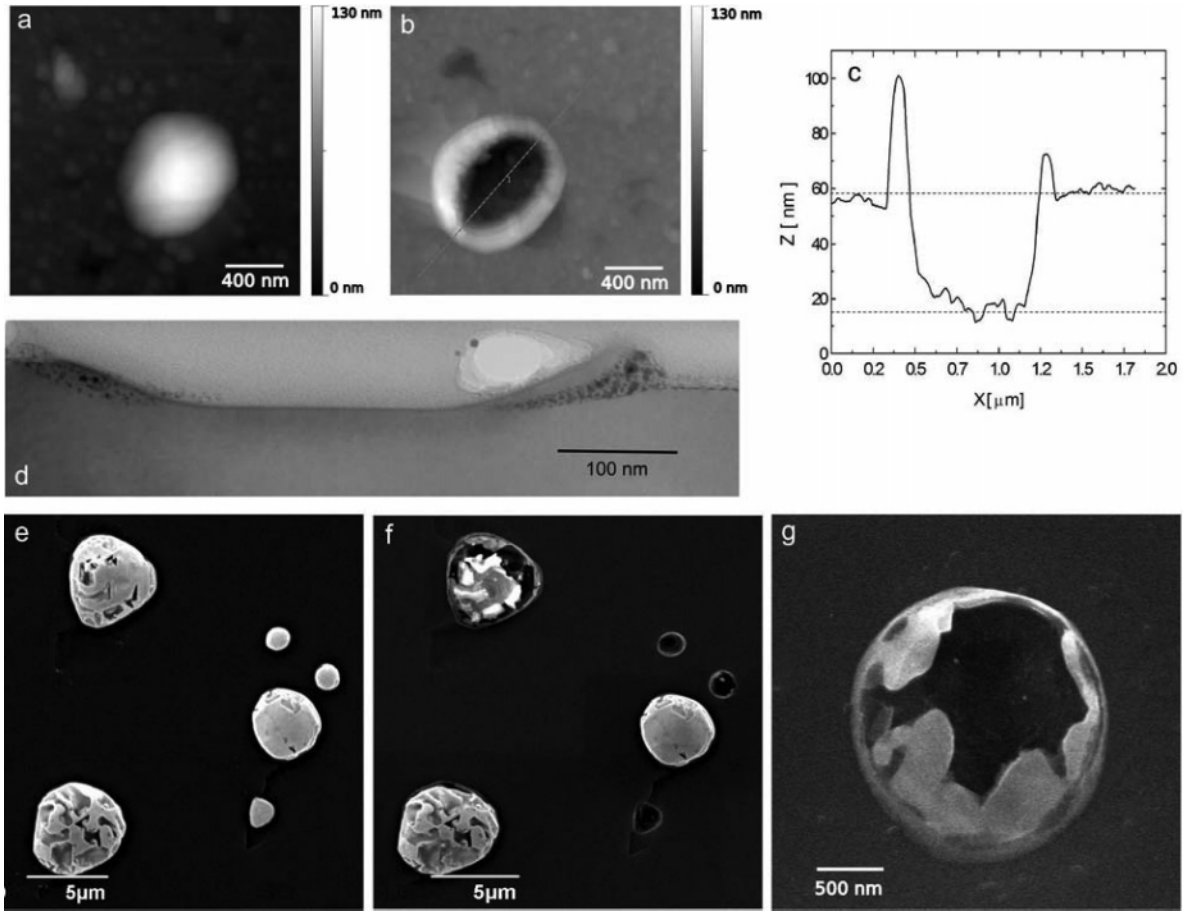

Figure 2. Effects of gold etching on the annealed Au/Si droplets: Atomic force micrograph (a) of a typical droplet obtained after annealing up to 827 °C and (b) of a droplet exposed to an iodine Au etch for 5 min. Both the profile across the droplet (c) and a cross-section transmission electron micrograph of a similar droplet (d) show the presence of a ring-shaped rim (∼25−40 nm in height) that surrounds a depression at the location previously occupied by the Au/Si droplet. The depth at the center of the depression is approximately ∼45−50 nm. Scanning electron micrographs of a set of droplets annealed at 827 °C are shown before (e) and after (f) the gold etch in iodine solution. While some of the droplets remain intact after the etch, others are emptied out. Cracks within the shell often allow the iodine to attack the Au core. Remnants of a cracked shell are shown in (g).

The correlation between the chemical composition of the 3D droplet and the specific annealing temperature is necessary to maintain the liquid−solid equilibrium at the interface. This is realized through Si incorporation in the 3D droplet from the substrate. Comparison of AFM images of the same droplets, acquired before and after the gold etching, allowed us to perform a volumetric analysis of the amount of Si incorporated in the droplets. We approximated the shapes of the droplet and of the depression to be that of a lens, with different radii of curvature. The presence of the rim, the debris of the nanoshell, and nanochannels (Figure 1b) limit the accuracy in the estimate of the depth of the depression, especially for droplets annealed at lower temperatures, whose depressions are shallower. We estimated the composition to change from the initial eutectic $Au_{81}Si_{19}$ to $Au_{63\pm2}Si_{37\pm2}$, upon annealing to T_F. (This composition is found to be independent of droplet size.) Following the liquidus line, this composition corresponds to the temperature of $T = 810 \pm 40$ °C. This is remarkably close to the annealing temperature $T = 827$ °C used during the experiment, considering both the experimental error in the temperature determination and the crude approximation used for the droplet shape and geometry. Similar analysis performed on samples annealed at 627 °C indicates a final composition of $Au_{73\pm2}Si_{27\pm2}$ and a nominal estimated temperature of $T = 570 \pm 50$ °C. Note that quenching the sample is critical to maintaining the composition of the droplet core close to the value reached upon annealing.

The fact that localized depressions are found provides evidence of pinning of the droplets to the substrate. The depressions beneath the droplets contribute to the pinning force/unit length of contact line by an amount that can be approximated as $F/L = \sigma[\cos\theta - \cos(\theta + \alpha)]$, where $\theta \approx 42°$ is the contact angle of the eutectic melt on flat substrate,[11] $\sigma = 780$ mN/m is the surface tension of the eutectic melt,[3] and $\alpha \approx 20°$ is the angle by which the substrate deviates from flatness under the droplets, measured by XTEM. Since σ varies weakly with temperature (and assuming, as is reasonable, that the same is true for θ), we estimate a contribution to the pinning force/unit length of about 214 mN/m at 827 °C. Note that such contribution is achieved only by annealing gold films well above the eutectic temperature. Indeed, the absence of depressions after the gold etch in films annealed to T_E indicates that Si dissolution from step edges into the droplets[11] occurs prior to or during the dewetting of the liquid melt. Thus, droplets of eutectic melt form without noticeable pinning at the surface, which favors their mobility and allows their coalescence in due time.[1]

However, pinning can be induced even at the eutectic temperature, if Au is deposited as isolated particles (Figure 1b). In this case, we find depressions in the substrate already at T_E.

This behavior is related to the negligible diffusion coefficient of Au on Si at these temperatures. Interestingly, surface diffusion of Au atoms (and, consequently, the establishment of the Au−Si intermetallic monolayer) does not set in until much higher temperatures are reached (>650 °C), regardless of the annealing time.[17]

Pinning of eutectic melt droplets provides an opportunity for nanopatterning, which can be useful, e.g., when Au nanoclusters are deposited on Si surfaces to catalyze the growth of Si nanowires.[18] Pinning of the catalyst stabilizes the pattern and prevents the clusters from coalescing. (Note, however, that the effect can be weakened if a gas phase source of Si is introduced *during* the anneal at high temperature, as gas phase incorporation may prevail over incorporation from the substrate.) In fact, the mechanism proposed herein explains why annealing to 877 °C prior to introduction of the precursor gas substantially preserved the original gold catalyst pattern in Si nanowires arrays, where uniformly dispersed gold nanoclusters were evaporated through the pores of an alumina template.[19] Faceting at the bottom of the depressions may be responsible for the actual direction of growth of Si and epitaxial III−V nanowires.[20]

As shown in Figure 2e,f, some droplets appear unaffected by the gold etch, which suggests the presence of a whole Si-rich shell sealing off the core. Around the eutectic temperature, we postulate surface crystallization of a Si-rich layer over a liquid Au−Si core to be the mechanism responsible for seeding the growth of these Si nanoshells. Surface crystallization of a Si-rich layer was observed recently in bulk eutectic samples near T_E.[3] Since near-surface enrichment in Si is driven by the lower surface tension of Si relative to Au, it is likely to persist even at higher temperatures. While the continuity of the shell in some droplets prevents the exposure of the Au−Si core to the gold etch, in those cases where the droplets are etched, the iodine attacks the Au core through cracks in the outer Si shell (Figure 2g). Presumably, these cracks form to relieve curvature stresses as well as stresses induced by the changes in temperature and volume of the liquid core, as it depletes of Si upon cooling.

As previously noted, Si enrichment in the composition of the droplets during high-temperature annealing is responsible for the formation of depressions underneath them and ultimately for the pinning of the droplets. Conversely, as the droplets are *slowly* cooled to the eutectic temperature, the composition of their core reverts to the equilibrium composition of the eutectic temperature, with excess Si expelled from the Au core. The persistence of deep depressions after the gold etch on the spots previously occupied by the droplets indicates that this excess Si does not refill such depressions. Instead, it goes to form the outer Si shell and in the larger droplets also to form Si channels that reach deep inside the core. The thickness of the Si shell depends on the maximum temperature reached during annealing. We observe that the rim of the droplets annealed at 827 °C is more pronounced and qualitatively thicker than the rim in samples annealed at 377 °C.

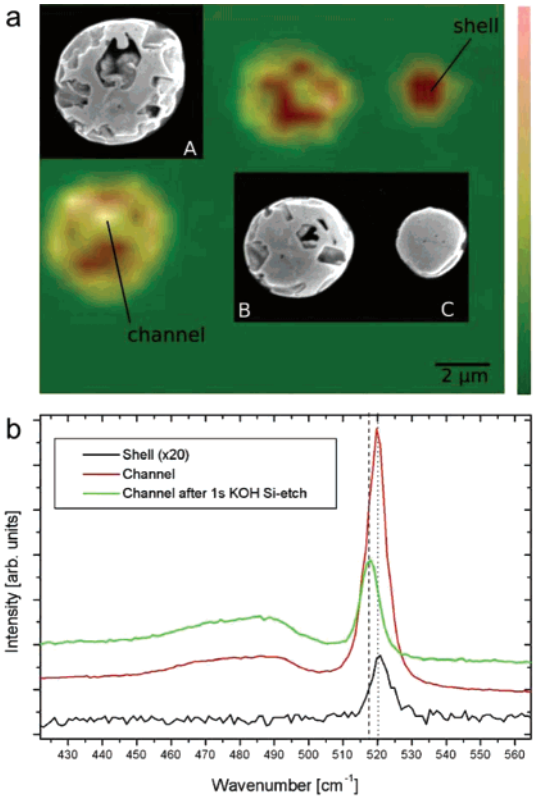

Figure 3. 3. (a) Raman micrograph of three droplets (with corresponding scanning electron micrographs) annealed at 727 °C. The intensities in the Raman map correspond to the integrated intensity of the sharp crystalline Si peak (520.5 cm^{-1} and a broad amorphous Si feature ~450−500 cm^{-1}). Higher intensities in the map (dark red/gray) correspond to Si rich areas. (b) Raman spectra of the nanoshell (black line, intensity magnified 20 times) and the Si-rich channels before (red line) and after the Si-etch in hot KOH (green line). A shift in the crystalline peak after the Si etch is visible in spectrum of the channels (518.7 cm^{-1}), due to the introduction of oxidation-induced stress during the etch.

Scanning confocal Raman microscopy (JY Horiba LabRAM in backscattering configuration; excitation line provided by a HeNe laser through an Olympus BX41 confocal microscope) was employed to investigate the crystal structure and homogeneity of the outer shells. Figure 3a shows a Raman map of three typical droplets (with corresponding SEM images in gray scale). The integrated intensity of the crystalline Si optical phonon peak (520 cm^{-1}) is represented in green−red (high−low) scale, while that of the broad amorphous Si band (~450−500 cm^{-1}) is represented in gray scale (white = high). The smaller droplet (C) appears homogeneous. The low intensity of the Si signal in the Raman map is simply a reflection of the fact that the photons originate above the eutectic core, and hence, only a small contribution from the outer crystalline Si shell is detected. A representative spectrum obtained on a point of the homogeneous shell is plotted in Figure 3b (black line).

In contrast to the homogeneity of the small droplets, larger droplets (A and B in Figure 3a) show pronounced chromatic variations, indicative of the existence of thick Si plates of crystalline and amorphous characters.[21] The presence of the latter is confirmed by the enhanced broad peak between ~450 and 500 cm^{-1}, in addition to the crystalline peak. A visual survey

(17) Slezak, J.; Ondrejcek, M.; Chvoj, Z.; Chab, V.; Conrad, H.; Heun, S.; Schmidt, T.; Ressel, B.; Prince, K. *Phys. Rev. B* **2000**, *61*, 16121.
(18) Gao, D.; He, R.; Carraro, C.; Howe, R. T.; Yang, P.; Maboudian, R. *J. Am. Chem. Soc.* **2005**, *127*, 4574−4575.
(19) Lombardi, I.; Hochbaum, A. I.; Yang, P.; Carraro, C.; Maboudian, R. *Chem. Mater.* **2006**, *18*, 988.
(20) Roest, A. L.; Verheijen, M. A.; Wunnicke, O.; Serafin, S.; Wondergem, H.; Bakkers, E. P. A. M. *Nanotechnology* **2006**, *17*, S271−S275.
(21) Smith, J. E., Jr.; Brodsky, M. H.; Crowder, B. L.; Nathan, M. I.; Pinczuk, A. *Phys. Rev. Lett.* **1971**, *26*, 642−646.

of several droplets imaged with SEM also indicates that while small droplets (such as droplet C) appear homogeneous, the larger ones present darker regions at their surfaces. Raman spectra acquired in the darker regions (Figure 3b, red line) show that the intensities of the crystalline and amorphous peaks are significantly enhanced compared to the regions with only thin shells, indicating a higher Si content and a deeper extent. These regions consist mainly of amorphous silicon, since the exposure of the droplets to a short (1 s) Si etch to remove top layers further increases the intensity of the amorphous peak over the crystalline peak by ~40% (Figure 3b, green line). In addition, the persistence of partially etched material after the short KOH etch indicates that, compared to the thin Si shell, such regions extend into the bulk of the droplets, creating Si-rich channels that pierce through the Au-rich core. A longer Si etch (30 s) leaves such channels completely empty.

The existence of the channels is due to phase separation of the binary alloy during cooling. Their extent depends primarily on the annealing temperature. When the cooling process starts from high temperatures, small Si-rich clusters nucleate within the core, as the droplets attempt to expel the excess Si. As the temperature is further decreased, the size of these clusters increases ultimately to form deep Si-rich channels. It is likely that when the channels reach the outer crystalline surface layer, a crystallization wave starts to propagate inward. This scenario is supported by the observation that the channels terminate near the surface into thick crystalline plates of regular shape (hexagonal or truncated hexagonal).

Conclusions

In conclusion, the dynamic readjustment of the chemical composition of the Au−Si clusters upon annealing induces structural and morphological changes in the AuSi clusters. Their Si enrichment from suitable annealing procedures affects the cluster/substrate morphology, with the result of pinning the clusters to the substrate and with the formation of Si nanoshells over the liquid eutectic core, induced by the surface crystallization of a liquid Au−Si alloy. A carefully programmed temperature sequence allows 3D gold droplets to be pinned at the surface with a degree of pinning force, which is uniquely dependent on the annealing temperature. In addition, it allows the production of thin Si nanoshells from nanostructured Au patterns. This could prove useful in sensing applications requiring microcavity environment and in nanofluidic applications involving controlled delivery.[22]

Acknowledgment. We acknowledge Gregory Doerk's assistance during SEM acquisition and Velimir Radmilovic for providing access to the National Center for Electron Microscopy facilities at the Lawrence Berkeley National Laboratory, which is supported by the U.S. Department of Energy under Contract No. DE-AC02-05CH11231. This work was supported by the National Science Foundation under Grant No. DMI-0304209, through the Center of Integrated Nanomechanical Systems.

Supporting Information Available: Auger electron spectra of Si(111) surface with dispersed Au particle before and after annealing to 1100 K; LEED pattern of the 6×6 reconstruction of the background Au monolayer; and geometry used to estimate droplet composition after annealing with parameters measured by SEM/TEM or AFM. This material is available free of charge via the Internet at http://pubs.acs.org.

JA7101983

(22) Sutter, P.; Sutter, E. *Nat. Mater.* **2007**, *6*, 363.